Project No. 01-59

PROPOSED ENHANCEMENTS TO PAVEMENT ME DESIGN: IMPROVED CONSIDERATION OF THE INFLUENCE OF SUBGRADE SOILS SUSCEPTIBLE TO SHRINK/SWELL AND/OR FROST HEAVE ON PAVEMENT PERFORMANCE

APPENDIX 9

STOCHASTIC FORECASTING OF TEMPERATURE AND THE THORNTHWAITE MOISTURE INDEX

MAY 2023

TABLE OF CONTENTS

9.0 STOCHASTIC FORECASTING OF TEMPERATURE AND THE THORNTHWAITE MOISTURE INDEX 9-4
9.1 Introduction 9-4
9.2 Deterministic Climate Model 9-5
Step 9.2.1: Weather Station Identification 9-6
Step 9.2.2: Monthly and 30-year Thornthwaite Moisture Index (Witczak et al., 2006) 9-7
9.3 Time Series Decomposition 9-8
Step 9.3.1: Stationarity, Transformations, and Autocorrelation, ... 9-8
Step 9.3.2: Transformations 9-9
Step 9.3.3: Autocorrelation 9-9
Step 9.3.4: Data Analysis via Decomposition 9-11
Step 9.3.5: Model Fit 9-12
Step 9.3.6: Model Validation 9-13
9.4 Review of Bayesian Forecasting Techniques 9-15
9.5 Markov Chain Monte Carlo (MCMC) Simulations 9-15
9.5.1 Time-Series MCMC 9-16
9.5.2 Variance Estimation 9-17
9.5.3 Initiating a MCMC Simulation 9-17
9.6 Time Series Decomposition of Monthly TMI Data 9-18
9.7 MCMC Framework for Stochastic Climate Parameter Forecasting 9-19
9.7.1 Stability and Optimization of Stochastic Climate Parameter Forecasting Model 9-21
9.7.2 Validation of Stochastic TMI Forecast Model 9-22
9.8 Performance of the Bayesian TMI Forecast Model 9-29
9.9 Stability of the Bayesian TMI Forecast Model 9-34
9.10 Potential Future Improvements to the Bayesian TMI Forecast Model 9-34
9.11 Limitations of the Bayesian TMI Forecast Model 9-34
9.12 References 9-36

LIST OF FIGURES

Figure 9-1: Paris, TX weather station (NOAA ID USC00416794) data from online TMI GIS map (Olaiz et al., 2017) ---------- 9-6
Figure 9-2: Monthly average temperature and rainfall data for NOAA weather station USC00416794 with the calculated yearly TMI (Witczak et al, 2006) between 9/1967 and 9/1997 ---------- 9-8
Figure 9-3: ACFs of TMI (Witczak et al., 2006) and dTMI for the TX 48-1068 SMP section from 3/1967 to 9/1997 ---------- 9-10
Figure 9-4: Time series decomposition of TMI and dTMI (black) showing moving average (MA in red) with lag = 12 and 3, respectively, and the associated monthly residuals (blue). ---------- 9-12
Figure 9-5: Known (posterior) data vs. model fit (forecasted) for TMI (top), dTMI (middle), and TMI moving average (MA) (bottom) ---------- 9-13
Figure 9-6: Histograms of monthly TMI vs. the MA (lag = 12) (top left), monthly dTMI vs. the MA (lag = 3) (top right), standardized monthly TMI vs. the MA (lag = 12) (bottom left), and standardized monthly dTMI vs. the MA (lag = 3) (bottom right).---------- 9-14
Figure 9-7 Procedure for Obtaining Monthly Parameterized Prior Distributions for the TMI MCMC Forecast Model---------- 9-20
Figure 9-8 Framework for monthly MCMC TMI forecast model using the Metropolis-Hasting Acceptance criteria. ---------- 9-21
Figure 9-9 Prior and Forecasted Monthly TMI from 03/2017 to 03/2022 for Arlington, VA (NOAA Station USW00013743)---------- 9-24
Figure 9-10 Prior and Forecasted Monthly TMI from 03/2017 to 03/2022 for Dallas, TX (NOAA Station USW00013960)---------- 9-25
Figure 9-11 Prior and Forecasted Monthly TMI from 03/2017 to 03/2022 for Denver, CO (NOAA Station USW00023062)---------- 9-26
Figure 9-12 Prior and Forecasted Monthly TMI from 03/2017 to 03/2022 for Salt Lake City, UT (NOAA Station USW00024127) ---------- 9-27
Figure 9-13 Prior and Forecasted Monthly TMI from 03/2017 to 03/2022 for Tempe, AZ (NOAA Station USW00013743)---------- 9-28
Figure 9-14 Histograms of Prior and Posterior (forecasted) Monthly Change in TMI for the Arlington, VA Validation Study Site from 03/2017 to 03/2022.---------- 9-30
Figure 9-15 Histograms of Prior and Posterior (forecasted) Monthly Change in TMI for the Dallas, TX Validation Study Site from 03/2017 to 03/2022. ---------- 9-31
Figure 9-16 Histograms of Prior and Posterior (forecasted) TMI for the Arlington, VA Validation Study Site from 03/2017 to 03/2022.---------- 9-32
Figure 9-17 Histograms of Prior and Posterior (forecasted) TMI for the Dallas, TX Validation Study Site from 03/2017 to 03/2022. ---------- 9-33

LIST OF TABLES

Table 9-1. Sites for Validation Study of the Proposed Stochastic TMI Forecast Model 9-22

9.0 STOCHASTIC FORECASTING OF TEMPERATURE AND THE THORNTHWAITE MOISTURE INDEX

9.1 Introduction

This document presents the calculation procedure for the time series decomposition and forecasting for the stochastic climate model. A computer program was developed using MATLAB to perform the calculation due to the multiple algorithmic processes required. The script file, with accompanying notes, is available and will be included in the final report.

The stochastic model builds upon the deterministic climate model approach presented previously in QPR5 in March 2020, and recently published by the group in the Soil and Rocks International Journal of Geotechnical and Geoenvironmental Engineering under the title "An improved framework for volume change of shrink/swell soils subjected to time-varying climatic effects" (Olaiz et al., 2021). The full publication is attached to this report. The Thornthwaite Moisture Index (Witczak et al. 2006) is used to quantity the climate for both, the deterministic and stochastic models.

Similar to the deterministic model, data from an AASHTO Long-Term Pavement Performance (LTPP) Seasonal Monitoring Program (SMP) section (TX 48-1068) approximately 80 miles northwest of Dallas, Texas (FHWA, 1995) is used to provide a real example of the calculation process.

The fundamental concepts of the stochastic climate model are based upon a modern time series concept, Bayesian inference, and a Markov Chain Monte Carlo (MCMC) iterative process. The initial time series analysis allows us to decompose the monthly TMI data into long-term/seasonal trends and unpredicted deviations from those trends, referred to as *noise* (Montgomery et al. 2016). Bayesian inference provides a reliable probabilistic approach that allows convergence to a targeted mean via several iterations of random samples drawn from the parameter space (Gelman et al. 2013). Most importantly, the MCMC technique allows for the random generation and estimation of data (Monte Carlo portion) which is dependent on the previously estimated value (Markov Chain portion). More specifically, the stochastic model proposed herein, utilizes a second-order moving average (MA(2)) of the monthly change in TMI (difference between the values of two consecutive months) to fit the historic data, and a permutation of the Adaptive Metropolis-Hastings (MH) algorithm (Metropolis et al., 1953; Hasting, 1970; Harrio et al., 2006) to forecast the expected TMI and its uncertainty. The proposed method utilizes the vast amount of stochastic time-series research used in the fields of climate change forecasting and stock market research.

The stochastic portion of the climate model including the MCMC simulation will be presented in a separate document due to its robust procedure. Although the stochastic portion of the new climate model

9.2 Deterministic Climate Model

Prior to initiating the stochastic climate model, the deterministic result must first be calculated. The deterministic process used for the calibration of the shrink/swell volume-change calculation incorporates the estimation of climate-induced time-varying suction changes at the surface boundary condition of the soil profile.

Within the procedure for calculating the time-varying volume change of shrink/swell soils, Olaiz et al. (2021) presented the following steps for the estimation of the site-specific time-varying surface suction:

1. Weather station identification and data extraction
2. Calculation of 30-year and monthly Thornthwaite Moisture Index per Witczak et al. (2006)
3. Determination of suction envelope parameters per Vann and Houston (2021) which includes the limits of suction variation at the surface
4. Initial estimation of monthly changes in suction at the surface as per Perera (2003)
5. Adjustment to the estimation of monthly changes in suction using limits of suction variation at the surface from Vann and Houston (2021)

Note that steps 3 and 5 use parameters that are based on the 30-year TMI value. Due to the nature of the proposed stochastic climate model, the 30-year TMI will change as each simulation randomly generates certain parameters. Therefore, steps 3 through 5 above will be performed following the generation of the stochastically forecasted TMI values. This report only presents the stochastic procedure for forecasting the time varying TMI. Steps 1 and 2 were extracted from Olaiz et. al (2021) and are presented herein as Steps 1.1 and 1.2.

The time series analysis continues from Step 1. A typical time series analysis adheres to the following process:

1. Problem understanding and data collection
2. Data analysis
3. Model selection and fitting
4. Model validation
5. Forecasting
6. Monitoring forecast performance
7. Updating forecast with new data

This report will discuss Steps 2 through 4. The forecast model, performance monitoring, and model updates will be discussed separately as these steps require a robust and adaptive feature to the proposed stochastic model.

Step 9.2.1: Weather Station Identification

An SMP pavement section approximately 80 miles northwest of Dallas, Texas (TX 48-1068) is used to provide an example for the proposed framework. For the purposes of this example calculation, the climate data was gathered from the weather station nearest to the site and identified using the open-access Thornthwaite Moisture Index (TMI) GIS map developed by Olaiz et al. (2017), which uses the National Oceanic and Atmospheric Administration's (NOAA) 30-year climate database for the United States. Figure 9-1 below presents an excerpt for the GIS map, which has the Paris, TX weather station selected.

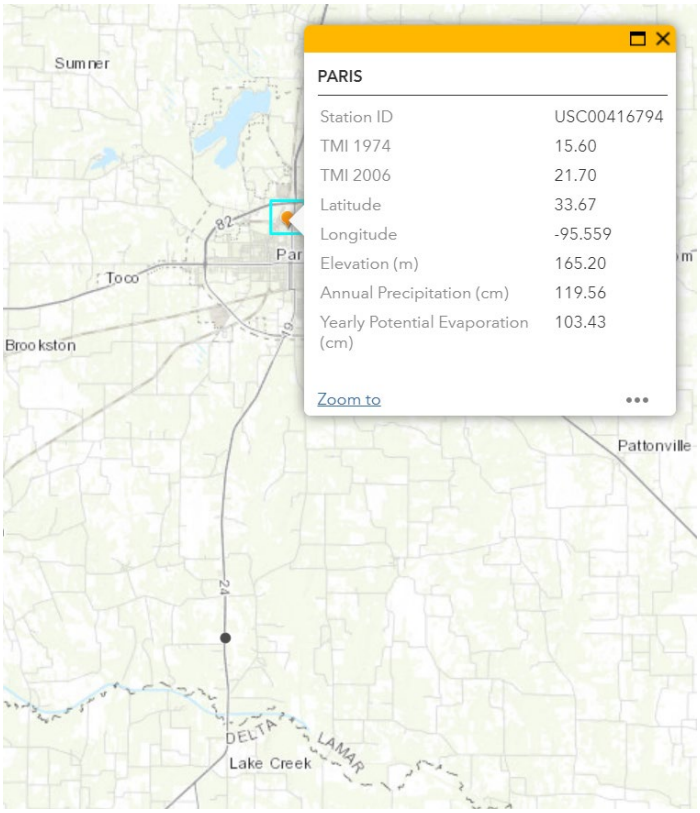

Figure 9-1: Paris, TX weather station (NOAA ID USC00416794) data from online TMI GIS map (Olaiz et al., 2017)

The "Station ID" shown in the pop-up window in **Figure** 9-**1** (USC00416794) is the only data needed as an input in the software product of this study. However, the remaining data shown may be helpful to get an understanding of the general climatic conditions at the site.

The NOAA climate data associated with each station in the country can be extracted from the online NOAA FTP site. It is recommended that the extracted weather data be filtered to contain the following variables, needed in the computation of the Thornthwaite Moisture Index (Witczak et al., 2006):

- Year

- Month
- Monthly Precipitation (cm)
- Monthly Average Temperature (Celsius)

Note that the Vann and Houston (2021) models used in the proposed analysis correlate the suction envelope parameters to a 30-year TMI value. As such, the climate data from the NOAA database for station USC00416794 was extracted for the date range of 9/1967 to 9/1997 (the last date of measured data from the SMP study for the TX 48-1068 section).

Step 9.2.2: Monthly and 30-year Thornthwaite Moisture Index (Witczak et al., 2006)

To determine a yearly TMI on a monthly basis, the potential evapotranspiration (*PET*) for each month must be calculated:

$$PET(cm) = f_1 f_2 1.6\left(\frac{10t}{I}\right)^a \tag{9-1}$$

Where, f_1 is the fraction of the number of days in month divided by the average number of days in month, 30; f_2 is the fraction of the number of hours in a day divided by the base of 12 hours in a day; t is the mean monthly temperature in degrees Celsius; I is the annual heat index; and a is a coefficient.

$$I = \sum_{i=1}^{12}\left(\frac{t_i}{5}\right)^{1.514} \tag{9-2}$$

where, t_i is the mean temperature for the i^{th} month, and

$$a = 6.75\times10^{-7}\left(H_y^{\,3}\right) - 7.71\times10^{-5}\left(H_y^{\,2}\right) + 0.017921\left(H_y\right) + 0.49239 \tag{9-3}$$

The TMI (Witczak et al., 2006) can now be determined by:

$$TMI = 75\left(\frac{P}{PET} - 1\right) + 10 \tag{9-4}$$

where, P is the precipitation for the given month.

To visualize the climate data over time, the monthly average temperature, the monthly rainfall, and the calculated TMI are plotted in **Figure 9-2**. For the example calculation at the TX 48-1068 SMP section, the 30-year weather data must be analyzed (9/1967 to 9/1997).

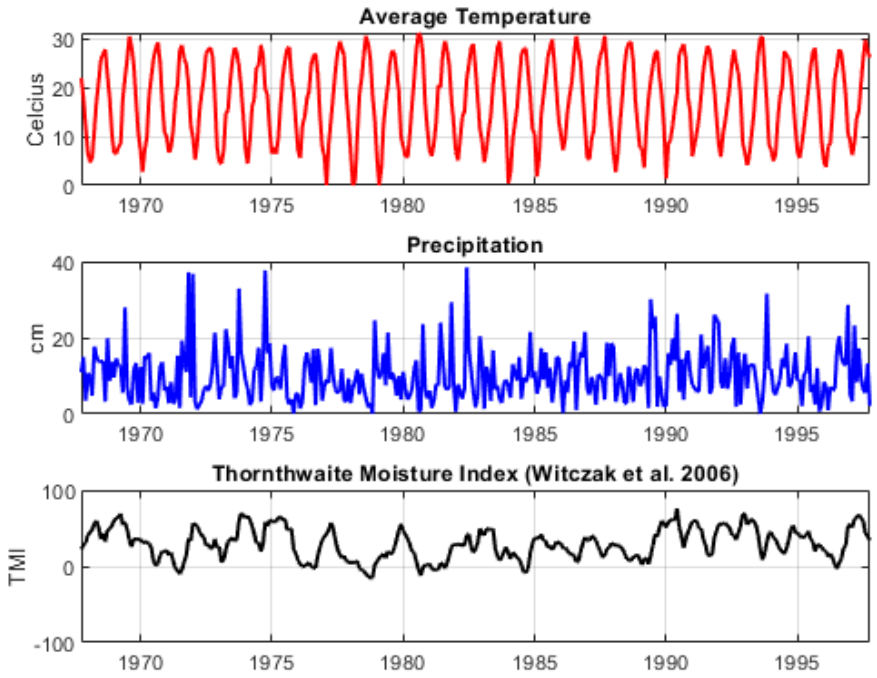

Figure 9-2: Monthly average temperature and rainfall data for NOAA weather station USC00416794 with the calculated yearly TMI (Witczak et al, 2006) between 9/1967 and 9/1997

The 30-year TMI value (Witczak at al., 2006) calculated from the NOAA data set for the USC00416794 station is +29.6. This value does differ slightly from the +21.7 value previously shown on the TMI GIS map for illustration purpose (**Figure** 9-**1**) due to the difference in date ranges used in the Olaiz et al. (2017) study.

9.3 Time Series Decomposition

The initial time series analysis gathered from the deterministic model must be decomposed into long-term/seasonal trends and the monthly deviations from those trends, referred to as *noise* (Montgomery et al. 2016). The time series decomposition includes stationarity tests, autocorrelation tests, determination of lag, and normality tests of the residual values to determine the most efficient model to fit the data. The stochastic model proposed herein utilizes a second-order moving average (MA(2)) of the monthly change in TMI (difference) to fit the historic data.

Step 9.3.1: Stationarity, Transformations, and Autocorrelation,

The first step of time series decomposition is to vary the stationarity of the data. Stationarity implies that the time series data moves around a relatively stable equilibrium or mean value. On the extreme side, strict stationarity indicates that the joint probability distribution at any time range

within the series is equivalent to a different time range within the series. General stationarity can be judged visually using a time series plot. The stationarity can also be judged mathematically using an autocorrelation approach. It is common to study both, the raw time series data as well as the smoothed/transformed time series data when determining stationarity, autocorrelation, and lag (time period associated with autocorrelated data).

Step 9.3.2: Transformations

Time series data is often transformed or adjusted to remove seasonal/long-term trends and to obtain a more stationary data set. A common form of transformation, used in the proposed forecasting model is *differencing*. Differencing is simply calculating the change between time steps, which can be represented using TMI as follows:

$$\Delta TMI_t = TMI_t - TMI_{t-1} \tag{9-5}$$

A second common transformation technique is to smooth the data using a moving average (M_T). The moving average represents the mean of the time series of a specified span (N). The moving average of the TMI at time period (T) is represented as:

$$M_T = \frac{TMI_T + TMI_{T-1} + ...TMI_{T-N+1}}{N} = \frac{1}{N}\sum_{t=T-N+1}^{T} TMI_t \tag{9-6}$$

The span of the moving average which provides the best fit to the data represents the lag term. The lag can be determined from a study of the autocorrelation functions.

Step 9.3.3: Autocorrelation

The covariance between the TMI at a given time (t) and the TMI a different time ($t+k$) is the autocovariance at lag (k), expressed as:

$$\gamma_k = Cov\left(TMI_t, TMI_{t+k}\right) = E\left[\left(TMI_t - \mu\right)\left(TMI_{t+k} - \mu\right)\right] \tag{9-7}$$

Where E represents the expected value of the expression. The autocovariance at zero lag ($k = 0$) represents the variance of the time series: $Var(TMI_t) = \gamma_0$. The autocorrelation coefficients (ρ_k) at any lag are expressed as:

$$\rho_k = \frac{Cov\left(TMI_t, TMI_{t+k}\right)}{Var\left(TMI_t\right)} = \frac{\gamma_k}{\gamma_0} \tag{9-8}$$

The autocorrelation functions (r_k) are then calculated by:

$$r_k = \frac{c_k}{c_0} \tag{9-9}$$

Where:

$$c_k = \frac{1}{T}\sum_{t=1}^{T-k}\left(TMI_t - \overline{TMI}\right)\left(TMI_{t+k} - \overline{TMI}\right) \tag{9-10}$$

And $c_0 = c_k\left(k=0\right)$, with $\overline{TMI}$ representing the mean of the TMI time series data.

The autocorrelation functions (ACFs) of the TMI and change in TMI (dTMI) data for the example TX 48-1068 SMP section from 3/1967 to 9/1997 are presented below.

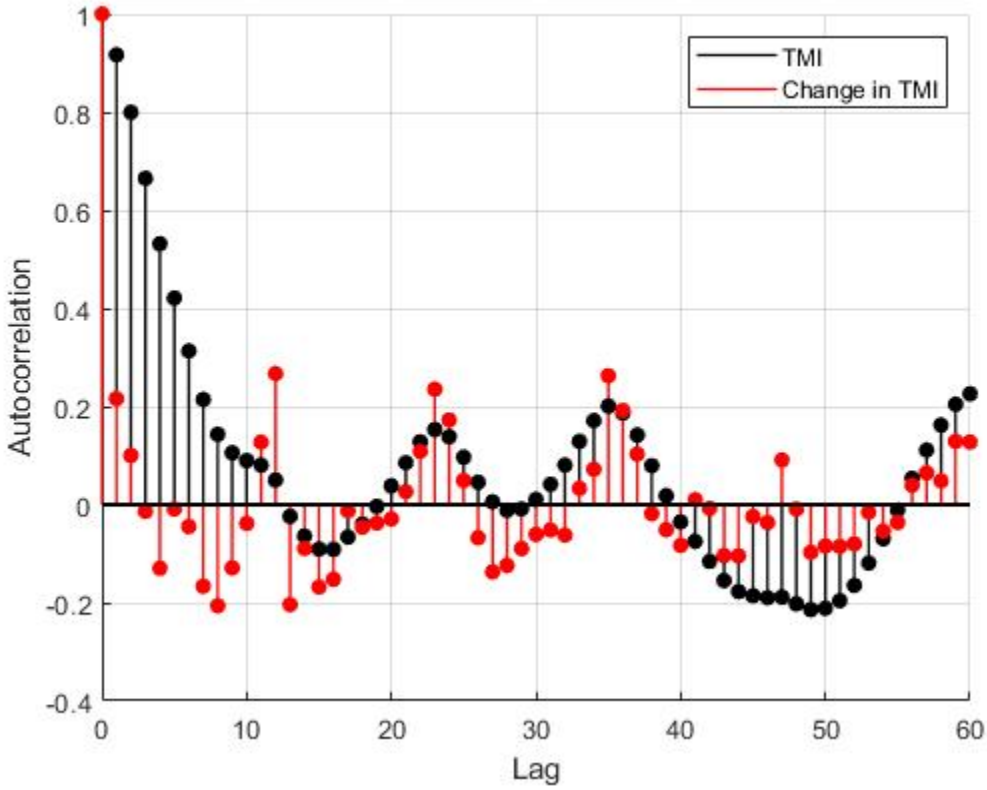

Figure 9-3: ACFs of TMI (Witczak et al., 2006) and dTMI for the TX 48-1068 SMP section from 3/1967 to 9/1997

Stationarity and lag can be visually interpreted from the ACF plot. Time series data, which exhibit stationary behavior, will have ACFs that decrease initially from 1 to approximately zero, and then will oscillate around zero, as both TMI and dTMI show, with minimal spikes above a specified

significance level (not shown above). The lag for both TMI and dTMI were determined by selecting where the ACFs just passed the zero value (TMI lag = 12, dTMI lag = 3). Note that the developed ACF values and plots were validated by the authors using the commercial statistical software Minitab.

Step 9.3.4: Data Analysis via Decomposition

Once stationarity of the time series data has been verified and the lag has been determined, the proper data transformation can be completed. Although there are several sophisticated time series data transformations (Montgomery et al., 2016), the TMI data has an inherent lag of 12 months due to its annual heat index, which allows a 12-span moving average to provide a reasonably good fit for most occasions. This phenomenon is evident in the previously presented ACF plot.

Generally, a time series (y_t) can be decomposed into a trend (T_t) component, a seasonal component (S_t), and a random error (noise) component (ε_t).

$$y_t = T_t + S_t + \varepsilon_t \tag{9-11}$$

A multiplicative model for time series decomposition is also frequently used although not presented herein. Due to the inherent yearly average of the heat index within the TMI calculation, the trend and seasonal component can be modeled together using a moving average of lag = 12 months ($M_{k=12}$). Therefore, the random noise for a given month of TMI (ε_t) data is expressed as:

$$\varepsilon_t = y_t - MA_{k=12} = TMI_t - MA_{k=12} \tag{9-12}$$

The figure below presents the time series decomposition of the TMI with lag = 12 months and dTMI with lag = 3 months. It is evident from the decomposition plots, that the differenced TMI data (change in TMI) has a better fit and lower magnitude in residual values than the raw TMI data. This provides enough evidence to choose a second order moving average (MA(2)) model (typically used when ACF has a lag = 3) of the change in (differenced) TMI.

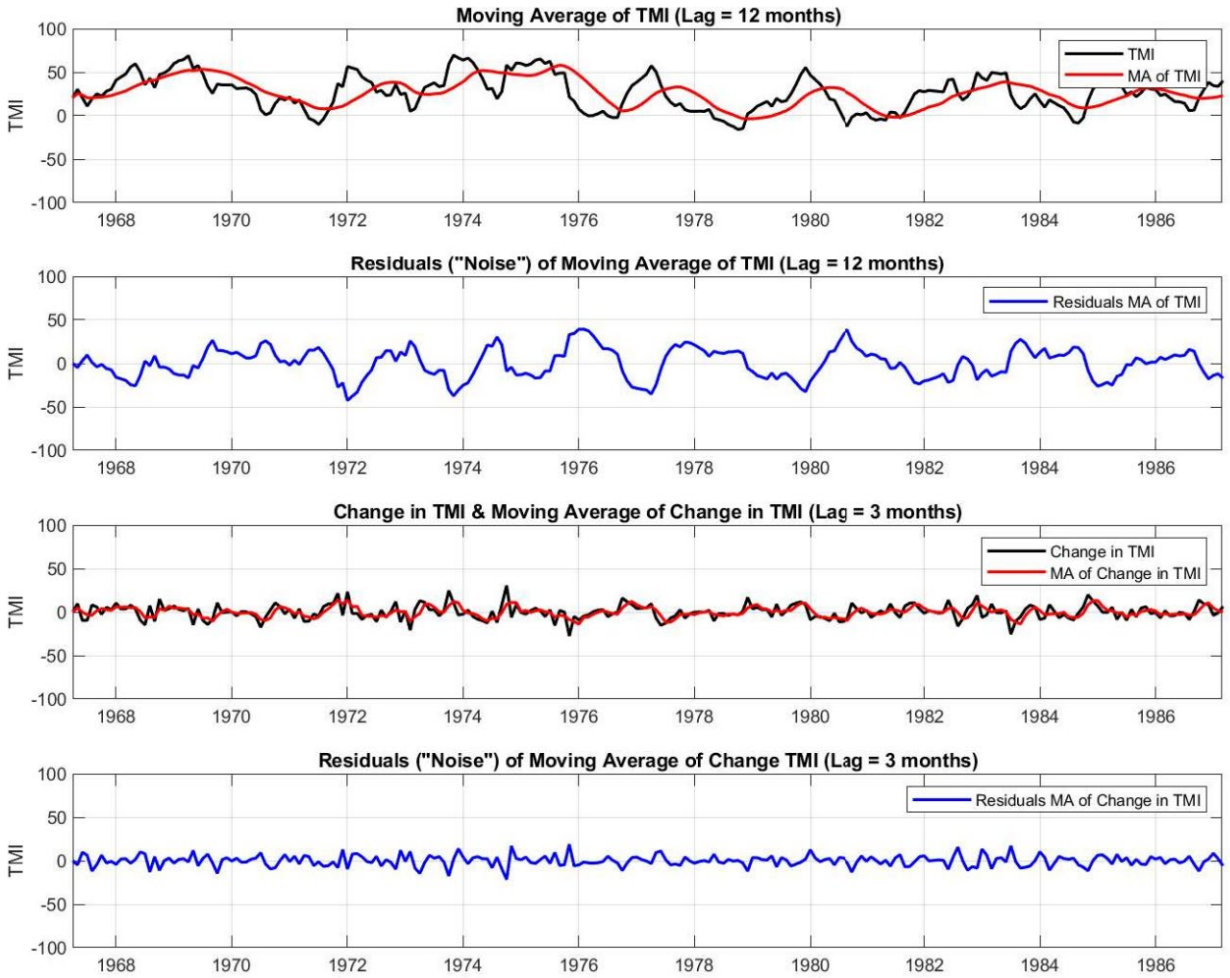

Figure 9-4: Time series decomposition of TMI and dTMI (black) showing moving average (MA in red) with lag = 12 and 3, respectively, and the associated monthly residuals (blue).

Step 9.3.5: Model Fit

The second order moving average (MA(2)) model of the differenced TMI (dTMI) is expressed as:

$$dTMI_t = \mu_{TMI} + \varepsilon_t - \theta_1 \varepsilon_{t-1} - \theta_2 \varepsilon_{t-2} \tag{9-13}$$

Where μ_{dTMI} is the average value of the sampled dTMI and represents the ACF parameters for dTMI at the lag identified by the subscripts. To improve the fit, the average value of the sample can be replaced by the moving average of the terms prior with lag = 3, as presented in the figure below. Note that once the dTMI value is estimated, the TMI term for a given month is calculated adding the change to the previous term, as expressed by:

$$TMI_t = TMI_{t-1} + dTMI_t \tag{9-14}$$

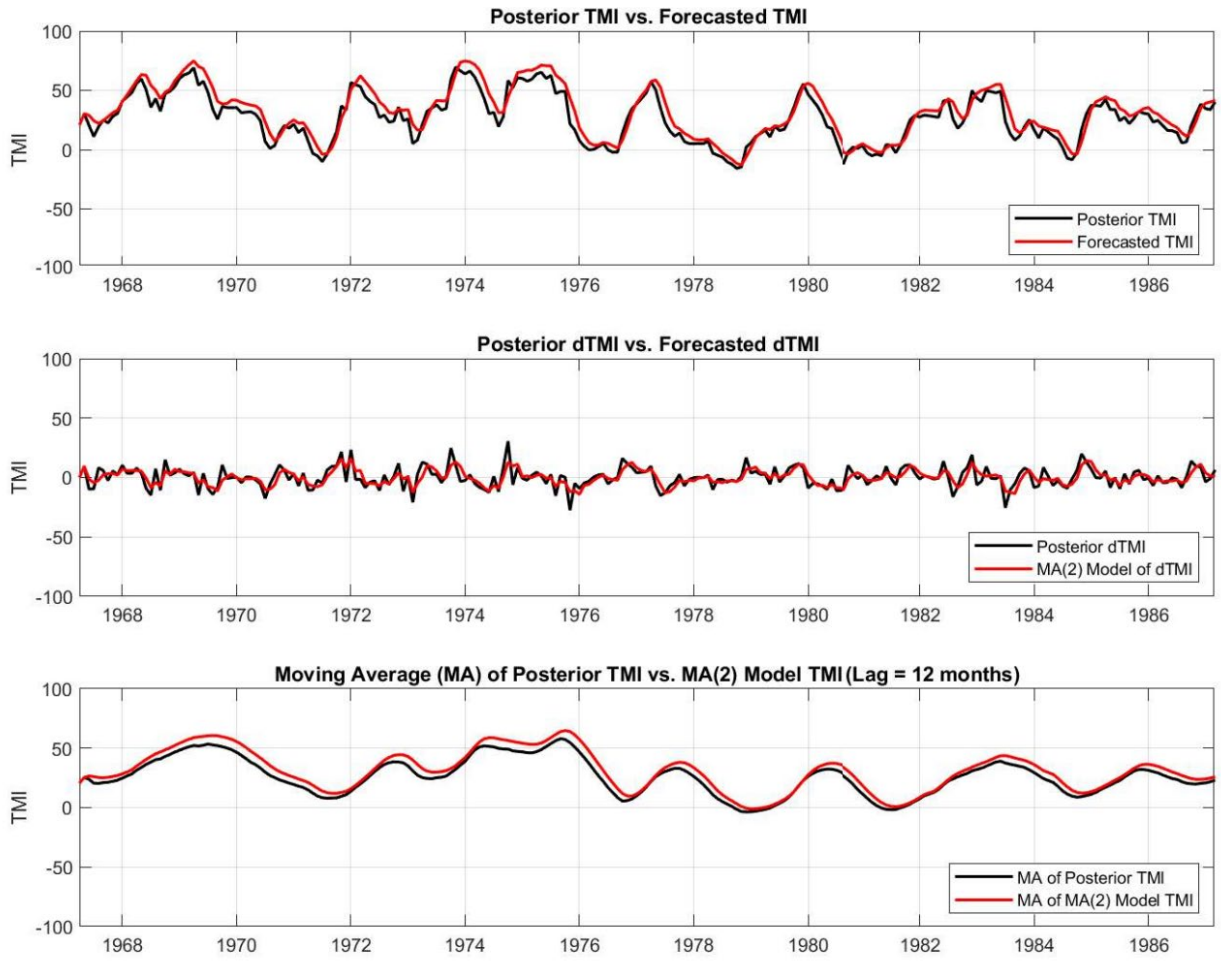

Figure 9-5: Known (posterior) data vs. model fit (forecasted) for TMI (top), dTMI (middle), and TMI moving average (MA) (bottom)

The dTMI model expressed in Eq. 13 will serve as the basis for the stochastic forecasting solution. However, the stochastic approach will incorporate the monthly statistics associated with each of the parameters in the equation (i.e., monthly means of dTMI, and autocorrelated monthly residual values).

Step 9.3.6: Model Validation

Validation of a good model fit of time series data is typically completed by studying the normality of the residuals, or noise. The figure below presents the histograms of the monthly TMI and dTMI residuals and the standardized residuals of each. Also presented on the histograms are normal probability density functions that were fit to the histogram data.

From the histogram plots, it is apparent that residuals of both moving average trends for TMI and

dTMI can be considered to follow a normal distribution. Typically, normality plots are developed to visually analyze the distribution of data. The author's generated normality plots using Minitab to validate the obvious interpretation of normality of the data from the histograms, although they are not provided in this report.

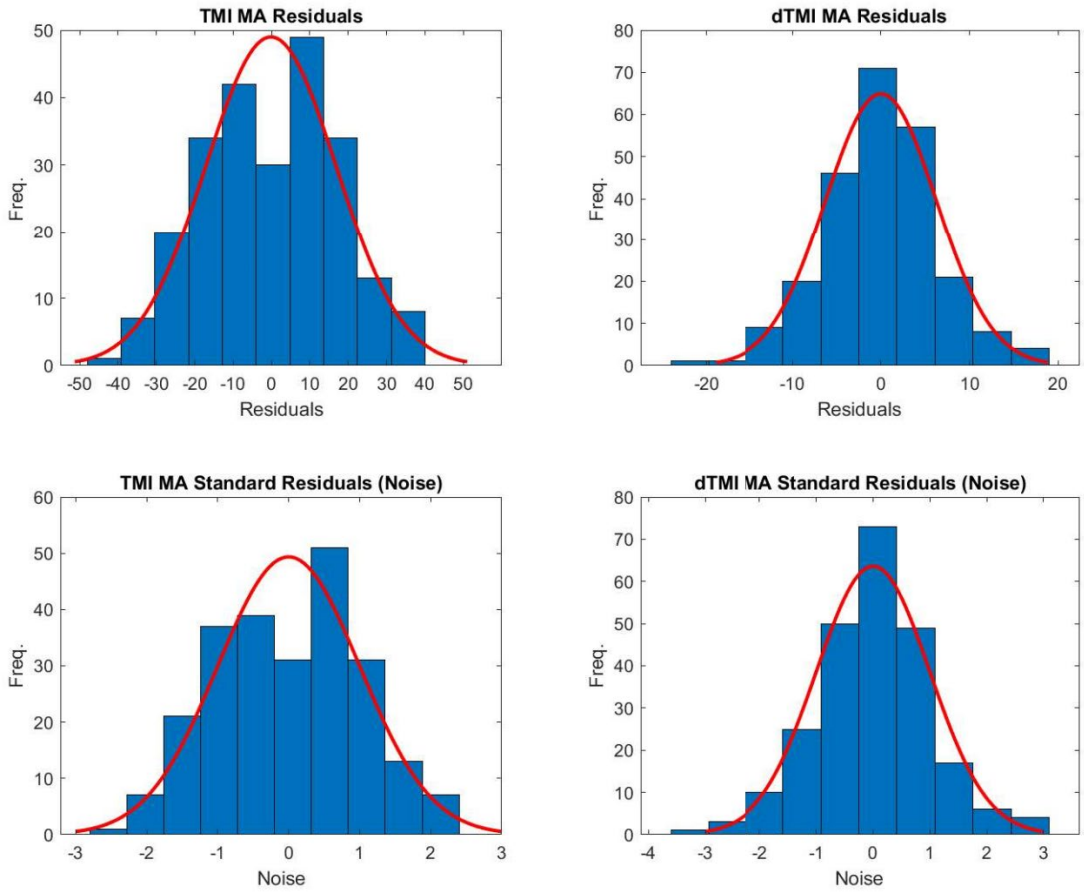

Figure 9-6: Histograms of monthly TMI vs. the MA (lag = 12) (top left), monthly dTMI vs. the MA (lag = 3) (top right), standardized monthly TMI vs. the MA (lag = 12) (bottom left), and standardized monthly dTMI vs. the MA (lag = 3) (bottom right).

9.4 Review of Bayesian Forecasting Techniques

Bayesian frameworks are a recent focus of study and implementation in geotechnical engineering (Zhang et al., 2004; Najjar and Gilbert, 2009; Ching et al., 2010; Chiu et al., 2012; Juang et al., 2013; Medina-Cetina and Esmailzadeh, 2014; Wang et al., 2016). However, the mathematical and computational complexity have limited the speed of adoption by the overall field (e.g., Zhang et al., 2009).

Prior knowledge and site/project specific data are used during geotechnical site characterization to estimate subsurface properties. The prior knowledge, or prior distribution, represents the estimation of the PDFs for the model parameters based on historical data/experience of similar parameters (e.g., the expansion potential of a fat clay at a new site is likely to be similar to other fat clays in the area or even around the world). The likelihood function is a key step in the Bayesian framework. The likelihood function is the PDF of site observation data for a given set of model parameters.

Bayesian framework are already being studied and implemented in in geotechnical engineering (Najjar and Gilbert, 2009; Ching et al., 2010; Chiu et al., 2012; Juang et al., 2013; Medina-Cetina & Esmailzadeh, 2014; Wang et al., 2016, Soltanpour, 2017). However, the mathematical and computational complexity have limited the speed of adoption by the overall field (e.g., Zhang et al., 2009).

It has been common practice to force normal distributions on prior and likelihood functions for the sole reason of convenience and simplicity. Although many geotechnical model parameters can pass a normality test, many will night and being able to represent the true variability of the model parameters (i.e. reflect the physical characteristics of the parameter) can have a significant effect of the model outcome.

9.5 Markov Chain Monte Carlo (MCMC) Simulations

One powerful tool in stochastic analyses and Bayesian Inference is the Markov-Chain Monte Carlo (MCMC) simulation, which can produce forecast estimates of highly correlated, multi-parameter, time-series data. MCMC forecasts data based on the conditional probability of observed (prior) data. Several recent publications which applied MCMC techniques to analysis of time series data and/or analysis of engineering related problems were reviewed as part of this study: Valdivieso (2009), Chen and Liu (2011), Sengupta et al. (2016), Bentancourt (2018), Koch et al. (2020), and Li et al. (2021).

A series of data is referred to as a Markov Chain is the conditional distribution of each time step is dependent or correlated to the previous time step. The general MCMC analysis approach involves a drawing proposal values unobserved data (θ^t) which is dependent upon or corrected by the previous draws (θ^{t-1}) so that a better representation of the target distribution is produced.

Markov Chains can be represented by the joint distributions of the given/observed data, referred to as the marginal distribution. Transition probabilities, or jumping distributions express the joint probability of the proposed variable at the current time step (θ^*) and the accepted variable at the previous time step (θ^{t-1}):

$$J^t\left(\theta^b \mid \theta^a\right) \equiv J^t\left(\theta^* \mid \theta^{t-1}\right) \tag{9-13}$$

Two common approaches are used in Bayesian inference to produce proposal variables and define criteria for acceptance and rejection of the proposed variables. One main goal of MCMC simulations is to create stationary Markov processes which results in the proposed variables falling within the distributions of the prior data for each sequential draw. The variance of a Markov Chain differs from the typical Monte Carlo simulation, or the good old-fashioned Monte Carlo (GOFMC) as defined by Geyer (). Due to the dependency on the previous data, the variance (σ^2) of a MCMC simulation, let's say $g\left(X\right)$, can be expressed as:

$$\sigma^2 = \operatorname{var}\left\{g\left(X_i\right)\right\} + 2\sum_{k=1}^{\infty}\operatorname{cov}\left\{g\left(X_i\right), g\left(X_{i+k}\right)\right\} \tag{9-14}$$

Where, *i* refers to the previous time current time step and k refers to either the previous or the future time steps (if the MCMC chain is reversible). Markov chains are not limited to representation of one variable at a time, but the general framework can apply to vectors and array variables as well. Furthermore, MCMC frameworks do not need to have stationary transition distributions; the variance and/or jumping distributions can be adaptive over time (Rosenthal, 2010).

9.5.1 Time-Series MCMC

Transitional probabilities for MCMC can also be defined by the autocovariance function, which is a common explanatory technique for time series analysis. The covariance function at any lag (*k*) can be expressed as:

$$\gamma_k = \operatorname{cov}\left\{g\left(X_i\right), g\left(X_{i+k}\right)\right\} = \frac{1}{n}\sum_{i=1}^{n-k}\left[g\left(X_i\right) - \hat{\mu}_n\right]\left[g\left(X_{i+k}\right) - \hat{\mu}_n\right] \tag{9-15}$$

Where *n* represent the total number of observations, $\hat{\mu}_n$ is the mean of the Markov Chain for an assumed normally distributed prior data set:

$$\hat{\mu}_n \approx \text{Normal}\left(\mu, \frac{\sigma^2}{n}\right) \tag{9-16}$$

1 Metropolis-Hastings

The key to performance of an MCMC simulation is the proposal mechanism and the acceptance/rejection process for the proposed sample. A common method to the

acceptance/rejection process is the Metropolis-Hasting (MH) approach. The MH techniques can be and are commonly combined with Gibbs sampling techniques to improve efficiency, usefulness, and computation time of the MCMC simulation. Originally, the Metropolis algorithm was as follows:

- Propose an unobserved data point ($\theta*$) given the conditional probability between either the prior or the accepted posterior distributions.

  $$p(\theta \mid y) \quad or \quad p\left(\theta^* \mid \theta^{t-1}\right)$$

- Calculate the Hastings Ratio:

$$r(y \mid \theta) \equiv r\left(\theta^{t-1} \mid \theta^*\right) = \frac{p(\theta)\, p(\theta \mid y)}{p(y)\, p(y \mid \theta)} \equiv \frac{p\left(\theta^*\right) p\left(\theta^* \mid \theta^{t-1}\right)}{p\left(\theta^{t-1}\right) p\left(\theta^{t-1} \mid \theta^*\right)} \qquad (9\text{-}17)$$

- Accept the proposed move to the variable ($\theta*$) if the $\min\left(1, r\left(\theta^{t-1} \mid \theta^*\right)\right) > u$.

The Metropolis-Hasting algorithm provided an update to the rejection aspect of the process and included the generation of a uniform random variable (u) between [0,1] following the calculation of the Hasting ratio.

9.5.2 Variance Estimation

The approach to represent the variance in MCMC simulations is a key factor which affects the performance of the model and can be represented/estimated in several ways. A batch sampling approach can be used which simply accounts for a finite number of samples, less than the total amount of samples, and assumes stationarity within the batch sample. Similar to a moving average approach, the variance within the batch sample is calculated and assumed to represent the posterior data at that time step. Batch sampling can include overlapping or not overlapping ranges of the sample data.

A second approach for defining the variance of time series data for MCM simulations is referred as the Initial Sequence Method and uses the autocorrelation function to represent dependency of the next time step on not only the typical lag data points, but also the period after the typical lag effect is negligible, and the period as the autocorrelation reverses to be opposite trend of the initial relationship.

9.5.3 Initiating a MCMC Simulation

One unfortunate aspect of MCMC models is that most useful models are developed and optimized to provide insight for a specific scenario and the application of each MCMC framework to other

applications is difficult.

Generally, a "Burn-in" or "warm-up" period is implemented into a MCMC model to allow for the posterior distributions to stabilize at or near the target distributions. Common practice when developing MCMC models is to start with a warm-up period that is 50% of the total number of simulations (Gelman et al., 2014).

This initial starting proposal point of an MCMC simulation can be chosen through a variety of approaches. The initial point can be a random draw from the prior distribution, or even the mean of the prior distribution can be used. The random draw of the posterior distribution can also be used, provided a warm-up period has been complete and the variance of the posterior distribution has stabilized. It there is a decent level of confidence in the prior distribution, or the prior data is highly correlated as with time-series data, a Gibbs sampling approach can be used to generate an approximation of the first proposal point.

9.6 Time Series Decomposition of Monthly TMI Data

The initial time series analysis gathered from the deterministic model must be decomposed into long-term/seasonal trends and the monthly deviations from those trends, referred to as *noise* (Montgomery et al. 2016). The time series decomposition includes stationarity tests, autocorrelation tests, determination of lag, and normality tests of the residual values to determine the most efficient model to fit the data. The stochastic model proposed herein, utilizes a second-order moving average (MA(2)) of the monthly TMI (moving average of the monthly change in TMI) to fit the historic data.

The second order moving average (MA(2)) model of the differenced TMI (*dTMI*) is expressed as:

$$dTMI_t = \mu_{TMI} + \varepsilon_t - \theta_1 \varepsilon_{t-1} - \theta_2 \varepsilon_{t-2} \qquad (9\text{-}18)$$

Where μ_{dTMI} is the average value of the sampled *dTMI* and represents the ACF parameters for *dTMI* at the lag identified by the subscripts. To improve the fit, the average value of the sample can be replaced by the moving average of the terms prior with lag = 3, as presented in the figure below. Note that once the *dTMI* value is estimated, the TMI term for a given month is calculated adding the change to the previous term. The *dTMI* model expressed in Eq. 104 will serve as the basis for the stochastic forecasting solution. However, the stochastic approach will incorporate the monthly statistics associated with each of the parameters in the equation (i.e., monthly means of *dTMI*, and autocorrelated monthly residual values). A visual example of the time series decomposition for using the MA(2) model of the monthly *dTMI* values is presented in Figure 9-7.

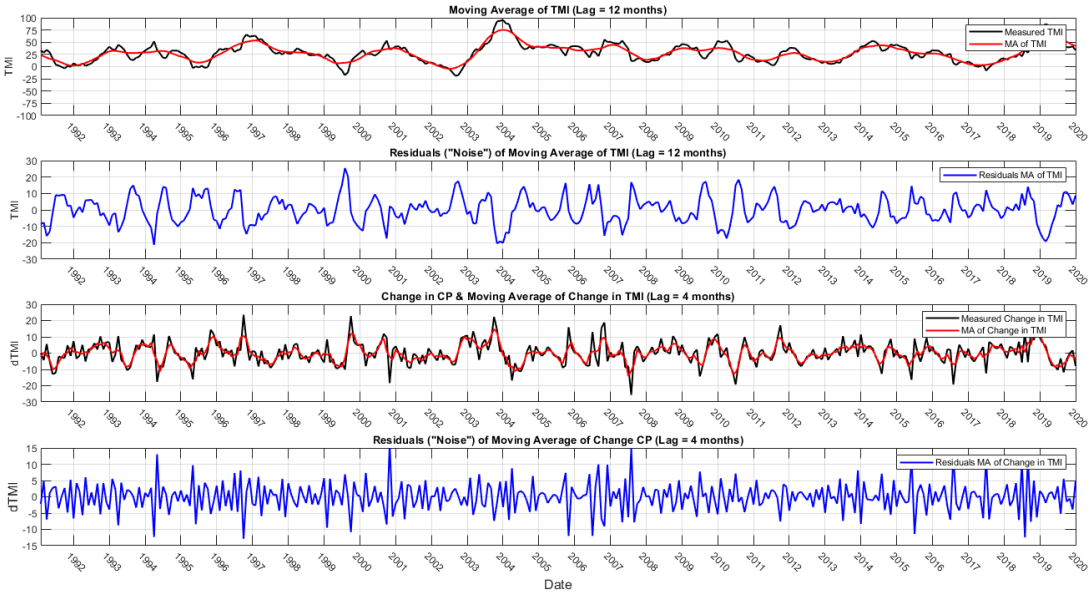

Figure 9-7 Time Series Decomposition of TMI and *dTMI* (black) using Moving Average (MA in red) with lag = 12 and 3, respectively, and the Associated Monthly Residuals (blue).

9.7 MCMC Framework for Stochastic Climate Parameter Forecasting

The monthly parameterized prior distributions for the MCMC TMI forecast model are obtained using the procedures presented in the diagram in Figure 9-8.

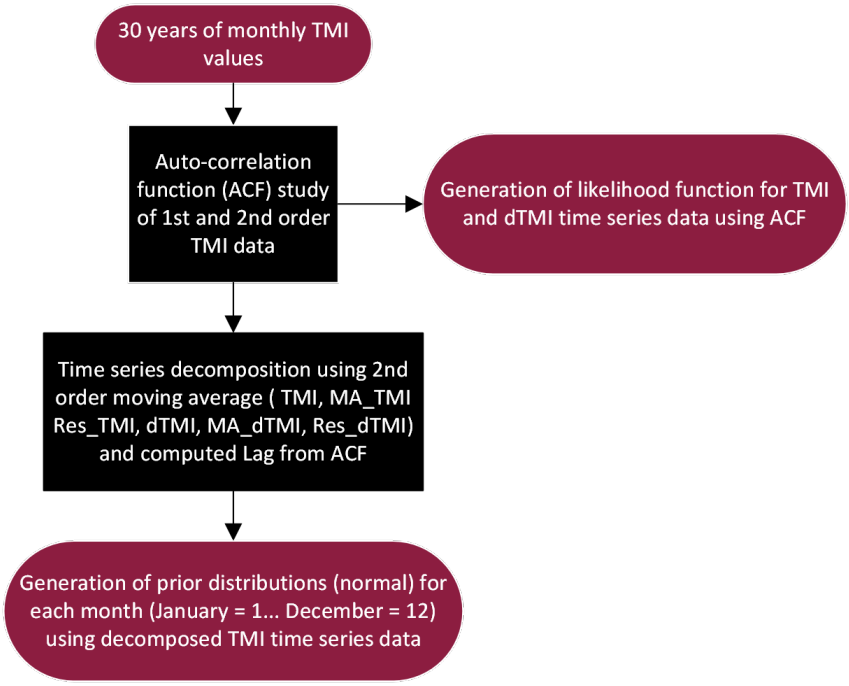

Figure 9-8 Procedure for Obtaining Monthly Parameterized Prior Distributions for the TMI MCMC Forecast Model

The overall framework of the MCMC algorithm using a Metropolis-Hastings acceptance criteria is presented in Figure 9-9.

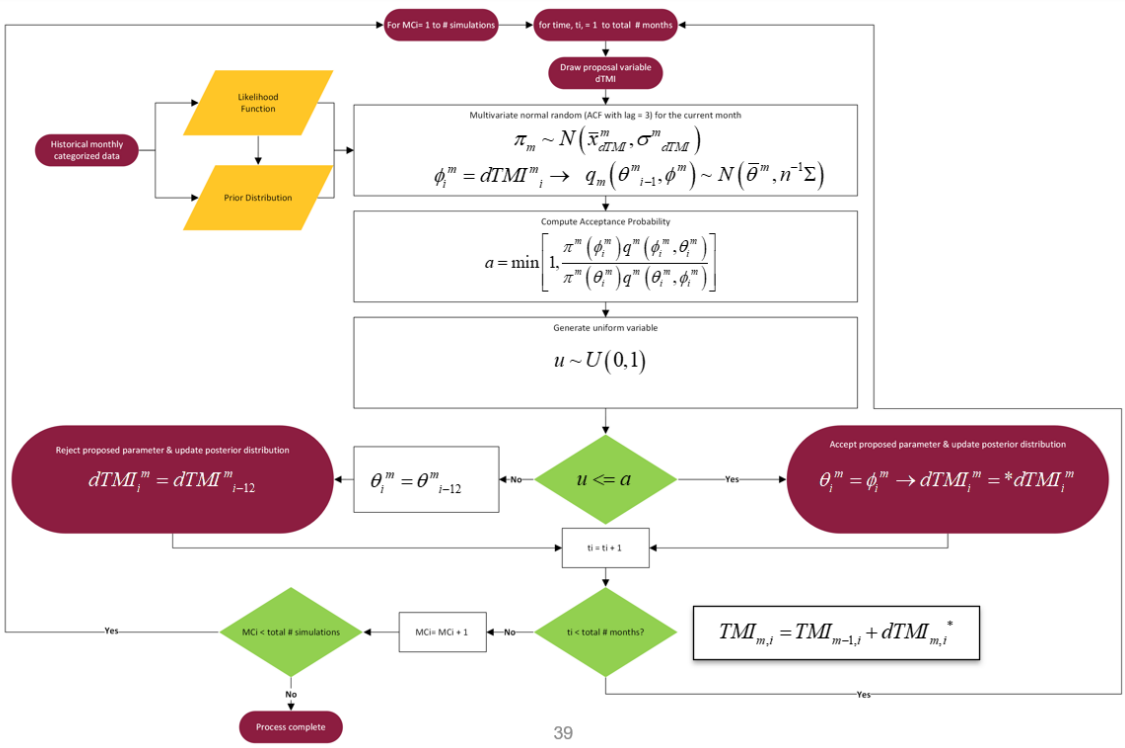

Figure 9-9 Framework for monthly MCMC TMI forecast model using the Metropolis-Hasting Acceptance criteria.

9.7.1 Stability and Optimization of Stochastic Climate Parameter Forecasting Model

The MCMC framework for stochastically forecasting the Thornthwaite Moisture Index went through numerous was optimized through numerous adaptations through iterations of trial and error until a useful model was obtained which could be efficiently applied to just about all locations in the US. The following concepts were incorporated into the analysis to help evaluate the stability and optimize the performance of the climate model.

- The generation of the proposal point initially began with a randomly generated value from the monthly parameterized prior distributions. To improve the efficiency and acceptance rate of the MCMC algorithm, a multivariate random number based on the posterior distributions within the lag period for *dTMI* is included in the final model. Frameworks which use Gaussian noise randomly generated number and the autocorrelation with the data points within the lag period was also explored but no benefit to the model performance was observed.
- The acceptance rate of Metropolis Hasting algorithm was calculated and evaluated to see if it fell within the typically accepted value for multidimensional models of 24%.
- A warm-up period was included in the algorithm which was set at 50% of the total simulations per recommendations by Gelman et al. (2014).

- An adaptive Metropolis-Hastings algorithm was developed which updated the target variance after a user-defined number of iterations to help drive and maintain the acceptance criteria around 24%. The adjustment factor and the update period were initially chosen to be 0.2 and 50 simulations based on recommendations by Vrugt (2016)
- Bounds of the posterior forecasted data were implemented on the TMI values, the moving average of the TMI, and the moving average of the change in TMI. The bounds were defined as three standards deviations on each side of the mean for the monthly parameterized prior data. The bound checks occur at each sequential time step and include a "step-back" process if the current proposal point falls outside of the bounds. On the time scale, the step-back period was set to be the lag of *dTMI* or *TMI* depending on which parameter had failed the bound checks. The implementation of the bound check and the step-back process is a rough approach to adding the benefit of a Hamilton Monte Carlo type algorithm without the direct inclusion of the energy expressions or the leapfrog algorithm.
- The Metropolis-Hasting algorithm was updated to include the conditional probability of the proposal TMI to help drive the posterior distribution of TMI closer to the target distribution and help improve stability of the model by reducing the variance of the posterior distribution of TMI.

9.7.2 Validation of Stochastic TMI Forecast Model

Five locations within differing climate regions were used to evaluate the performance of the TMI forecast model. The simulated time period was from March 2017 to March 2022 (5 years). By using a forecast window of historical data, a comparison can be made between the forecasted TMI and the actual TMI during that period. Note that the historical data during the comparison period was not included in the prior distributions. Thirty years of prior climate data from NOAA was collected and used to develop monthly distributions for *TMI*, *dTMI*, *TMI_MA*, and *dTMI_MA*. Using a monthly-based component-wise setup allows for the qualitative knowledge that weather data is typically similar in each month year after year; however, the monthly component-wise setup limits the number of data points for each component distribution to the number of years of historical data available at the site. The five locations used for evaluation of the proposed TMI forecast model are presented in Table 9-1 along with the NOAA weather station ID, the 30-year TMI, and the climate region as defined by AS2870 (2011).

Table 9-1. Sites for Validation Study of the Proposed Stochastic TMI Forecast Model

Location	NOAA Weather Station (ID#)	30-Year TMI	Climate Region*
Arlington, VA	Washington Reagan Airport (USW00013743)	24	Wet Coastal / Alpine

Location	NOAA Weather Station (ID#)	30-Year TMI	Climate Region*
Dallas, TX	Dallas FAA Airport (USW00013960)	-5	Wet Temperate to Temperate
Denver, CO	Denver Central Park (USW00023062)	-19	Dry Temperate
Salt Lake City, UT	Salt Lake City International Airport (USW00024127)	-26	Semi-Arid
Tempe, AZ	Phoenix Sky Harbor International Airport (USW00013743)	-58	Arid

* As defined by AS2870 (2011) based on TMI

The autocorrelation functions, histograms, and boxplots of the parameterized data of the monthly TMI time-series decomposition and the MCMC forecasted TMI for the five locations are presented in Appendix E. The results of the TMI forecast for Arlington, VA, categorized as a wet coastal/alpine climatic region, are presented in Figure 4-5. The results of the TMI forecast for Dallas, TX, categorized as a Temperate to Wet Temperate climatic region, are presented in Figure 4-6. The results of the TMI forecast for Denver, CO, categorized as a dry temperate climatic region, are presented in Figure 4-7. The results of the TMI forecast for Salt Lake City, UT, categorized as a Semi-Arid climatic region, are presented in Figure 9-10. The results of the TMI forecast for Tempe, AZ, categorized as an arid climatic region, are presented in Figure 9-11. The figures present the prior data, the forecasted data, and the true data within the forecast period for comparisons and validation purposes.

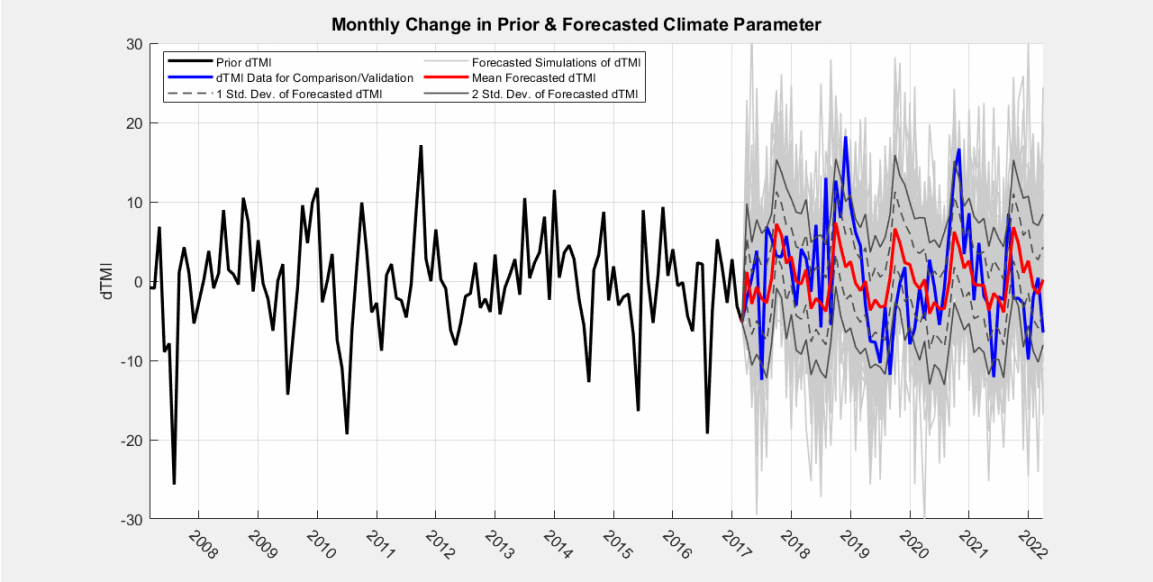

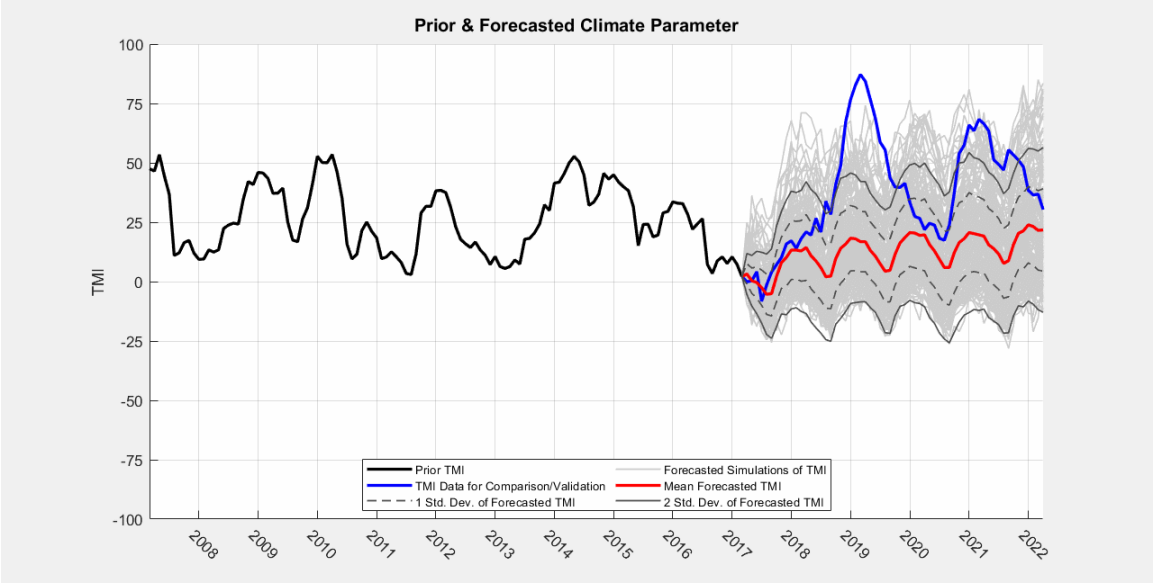

Figure 9-10 Prior and Forecasted Monthly TMI from 03/2017 to 03/2022 for Arlington, VA (NOAA Station USW00013743)

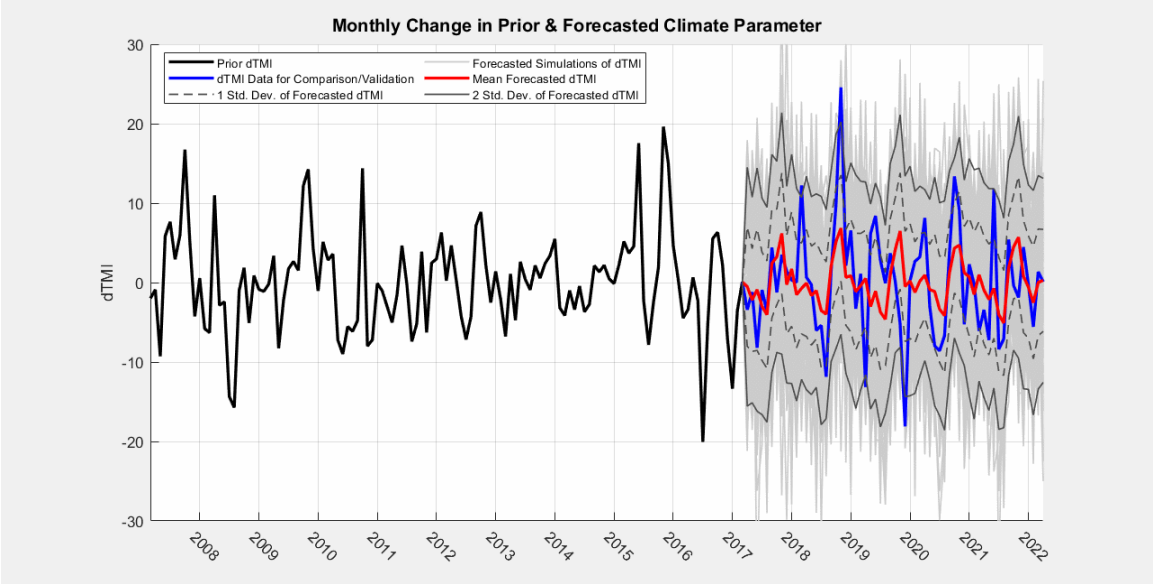

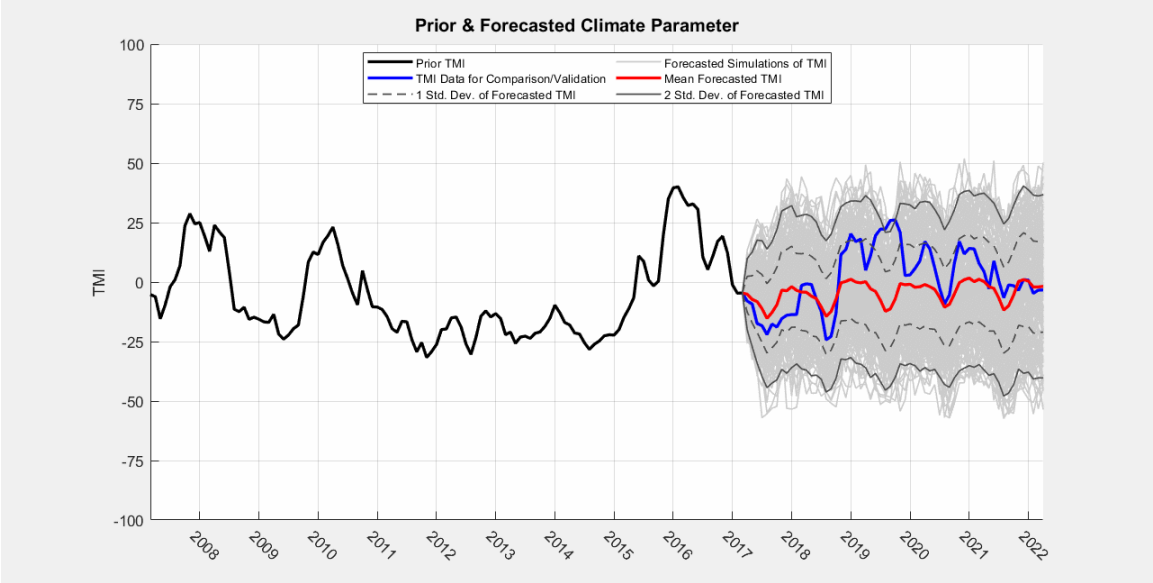

Figure 9-11 Prior and Forecasted Monthly TMI from 03/2017 to 03/2022 for Dallas, TX (NOAA Station USW00013960)

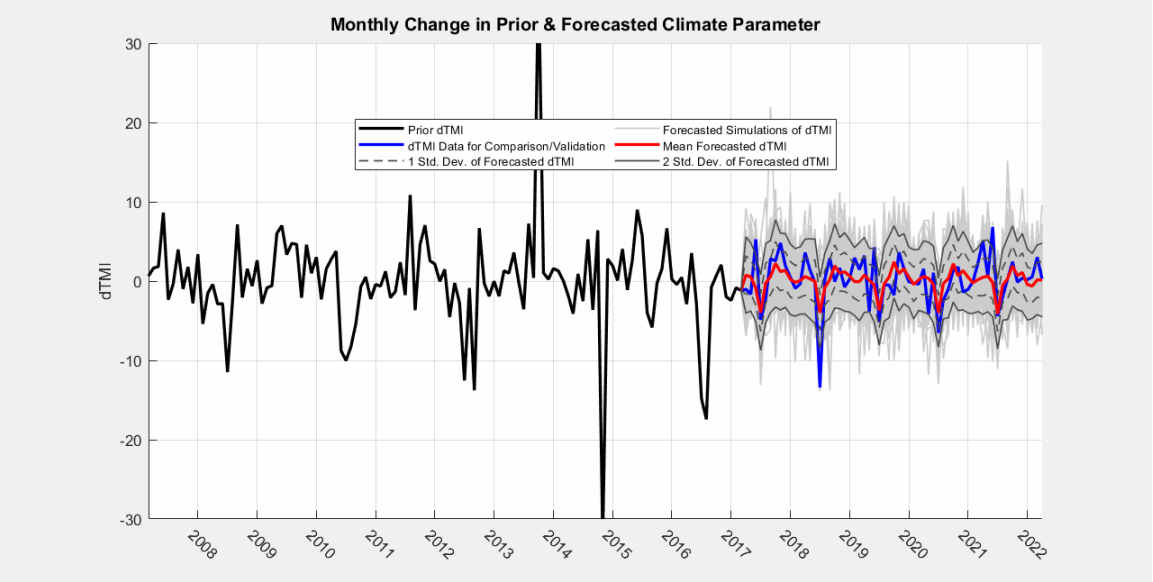

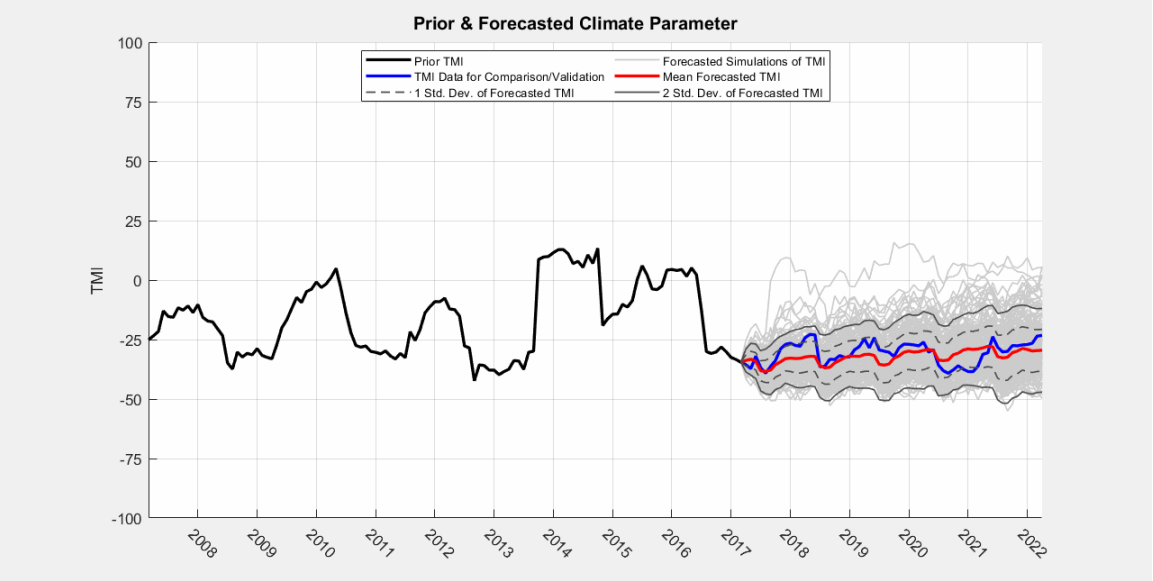

Figure 9-12 Prior and Forecasted Monthly TMI from 03/2017 to 03/2022 for Denver, CO (NOAA Station USW00023062)

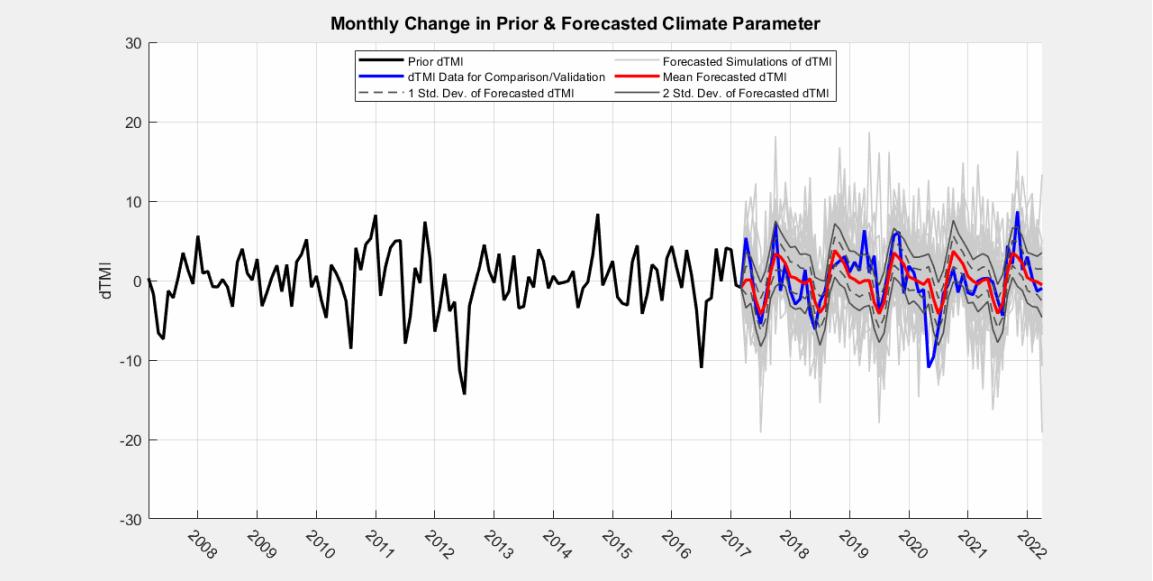

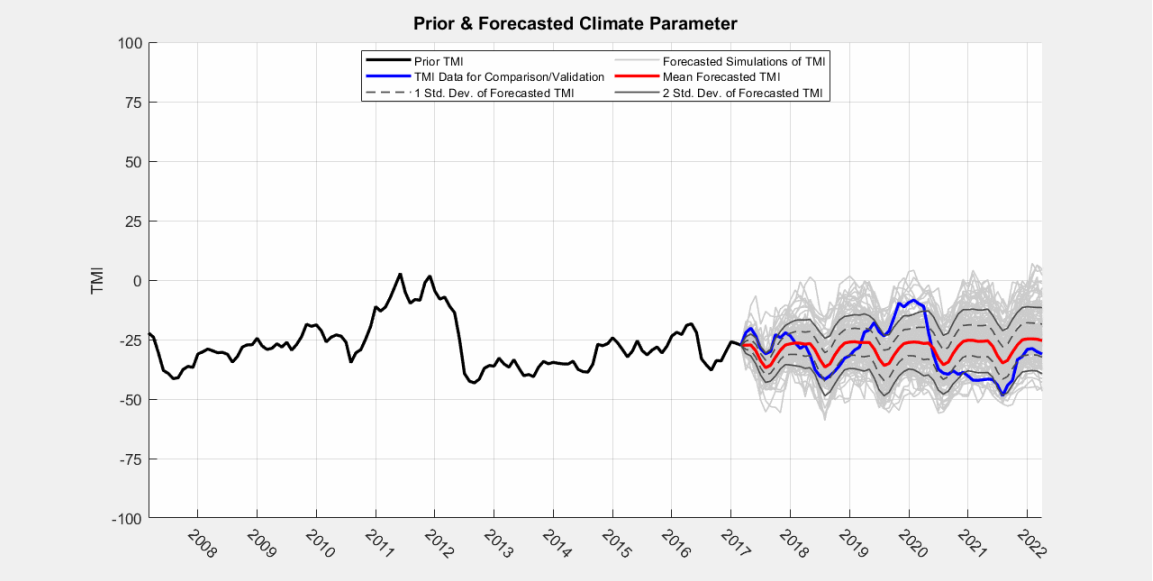

Figure 9-13 Prior and Forecasted Monthly TMI from 03/2017 to 03/2022 for Salt Lake City, UT (NOAA Station USW00024127)

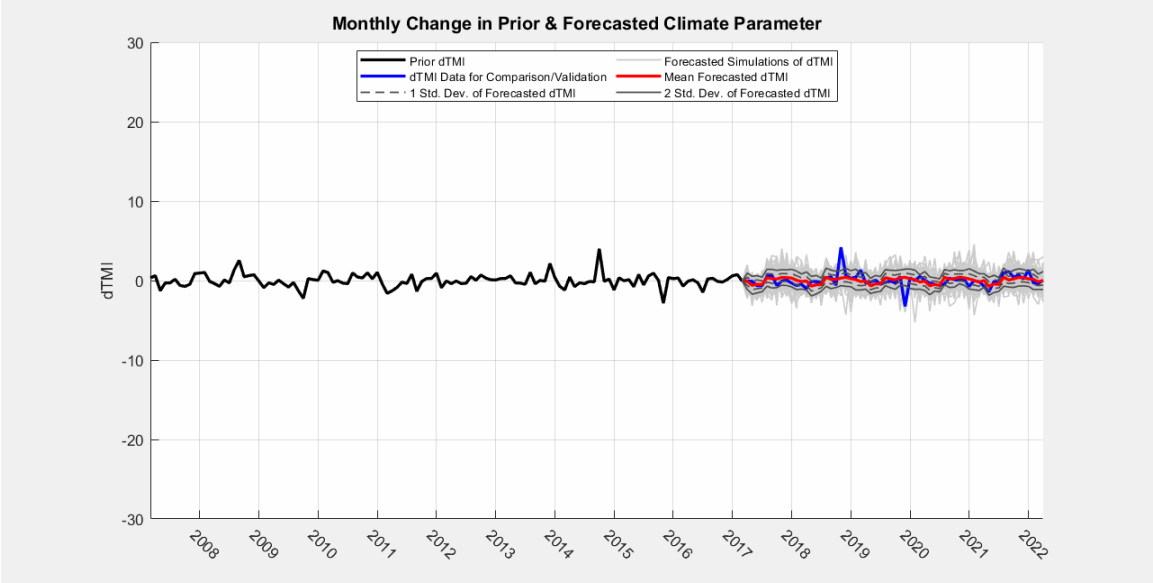

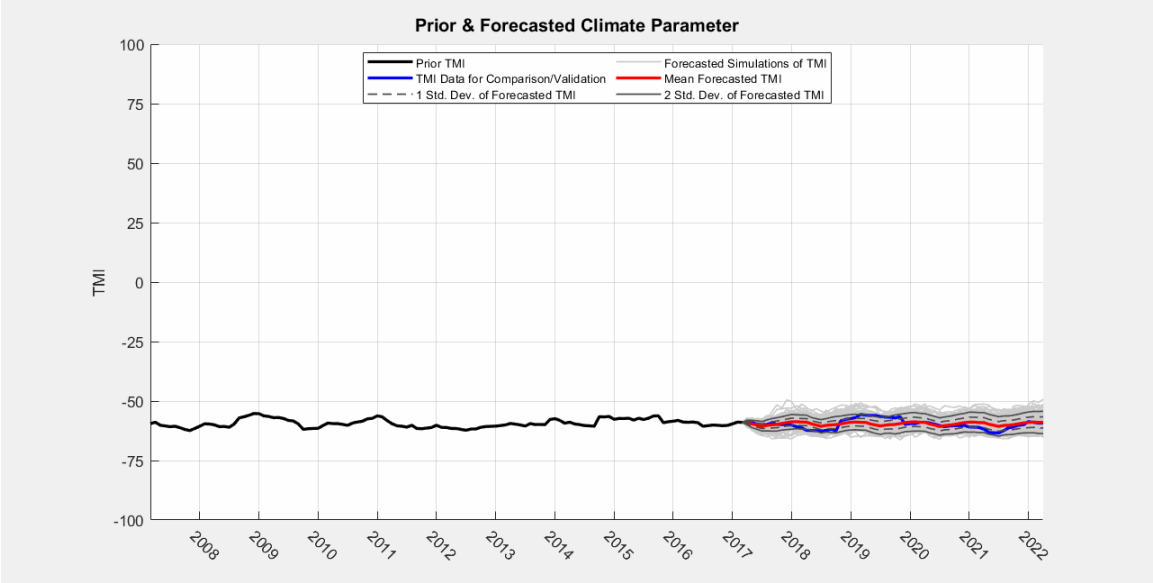

Figure 9-14 Prior and Forecasted Monthly TMI from 03/2017 to 03/2022 for Tempe, AZ (NOAA Station USW00013743)

Based on a visual evaluation of the forecasted TMI and monthly change in TMI of the five locations presented in Table 9-1, the following conclusions cans be made regarding the validation of proposed model.

- The prior TMI data (30 years) of the wet coastal/alpine location in Arlington, VA exhibited relatively high seasonal variation. The forecasted *dTMI* captures most of the true data within one standard deviation from the forecasted mean and nearly all of the extreme values of the true data are captured within two standard deviations from the forecasted mean. The individual forecasted chains of *dTMI* resulted in show that there were several forecasted chains which consisted of extreme values greater than both the prior data and the true data within the forecast period. Although the *dTMI* forecast provides adequate representation of the true data and the variability of the prior data, the TMI forecast fails to encompass the extreme wetting period between 2017 and 2020 within two standard deviations of the mean, which is most likely caused by this period exhibiting TMI values higher than data from the 30 years of prior data.
- The example forecast for the wet temperate to temperate location in Dallas, TX resulted in a relatively better fit to the true data. Although the *dTMI* forecast does not fully capture all extreme values within two standard deviations from the mean, the corresponding TMI forecast data does encompass the extreme events within 2 standard deviations. This improvement may be due to the four years of relatively dry (low) TMI values followed by a two-year period of wetter (increased) TMI values just before the start of the forecast period. Additionally, the period of wetting prior to the forecast period consists of higher TMI values that the true data within the forecast period. Overall, the Bayesian TMI forecast

model for this example location in a wet temperate to temperate climate region produces forecasted values which adequately represent the variability of the prior data and encompassed the potential extreme events.

- The example forecasts for the dry temperate and semi-arid locations of Denver, CO and Salt Lake City, UT, respectively, produced promising results for the forecasted dTMI and TMI data. The moving of the forecasted *dTMI* is similar to the true values within the forecast period with the exception of a few extreme values. The standard deviations of the forecasted *dTMI* data are much closer to the mean values, compared to the wet coastal/alpine and wet temperate to temperate examples. This reduction in forecasted variability is also observed on the forecasted TMI plots, without a noticeable reduction in the over forecast performance. Most of the true TMI data for both the dry temperate and the semi-arid example are encompassed within one standard deviation from the forecasted mean with the exception of one extreme period in the Salt Lake City example from 2019 to 2020, which falls just outside two standard deviations from the forecasted mean.
- The example forecast for the arid location of Tempe, AZ also produced a relatively good fit to the true data, although the variability and volatility in both TMI data for this climate region was minimal.

9.8 Performance of the Bayesian TMI Forecast Model

Overall, the visual evaluation of the Bayesian TMI forecast model for the five locations explored herein provide an adequate job of producing forecasted data which exhibit near the same seasonal averages and monthly variation as the prior and the true data within the forecast period. The forecast model appeared to perform best for the dry temperate and semi-arid locations which is a promising outcome for the potential implementation for unsaturated soil shrink-swell volume change analysis as these climate regions are commonly associated with expansive soil related issues to infrastructure. The performance of the model in the arid region is tough to evaluate using the Tempe, AZ example as the variability of the prior data was minimal. It appears that the climate within this region is relatively stable which would indicate that the issues with shrink-swell soils would be governed by extreme events and not the natural seasonal moisture variations.

To further evaluate the performance of the Bayesian TMI forecast model, the histograms of the monthly parameterized priors and posterior (forecasted) *dTMI* and TMI values were generated and are presented in Appendix E for each of the five locations used in the validation study. Figure 9-15 and Figure 9-17 present the *dTMI* and TMI prior and posterior histograms, fitted with normal distributions, for the Arlington, VA validation study location, respectively. Figure 9-16 and Figure 9-18 present similar data for the Dallas, TX validation study location.

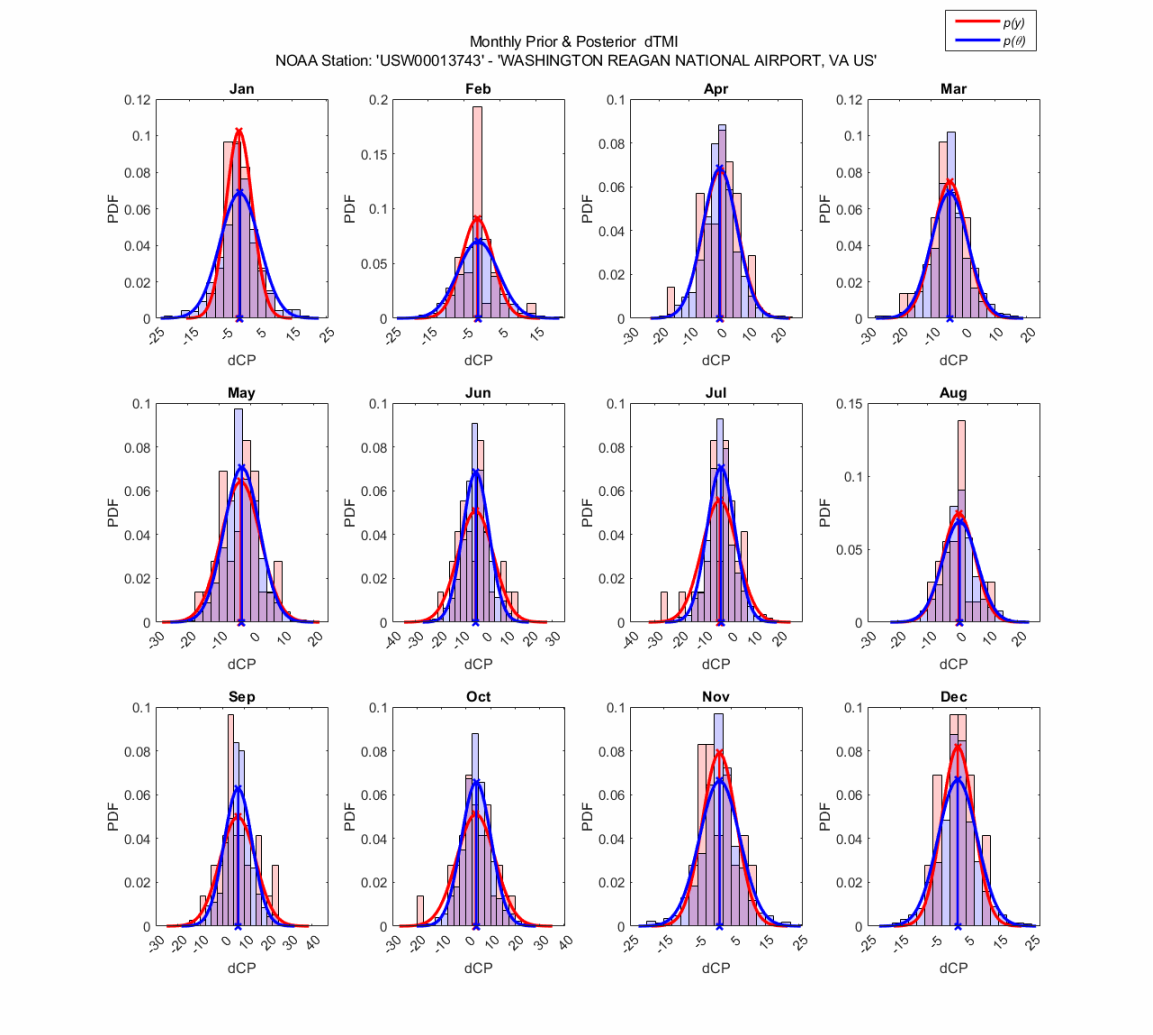

Figure 9-15 Histograms of Prior and Posterior (forecasted) Monthly Change in TMI for the Arlington, VA Validation Study Site from 03/2017 to 03/2022.

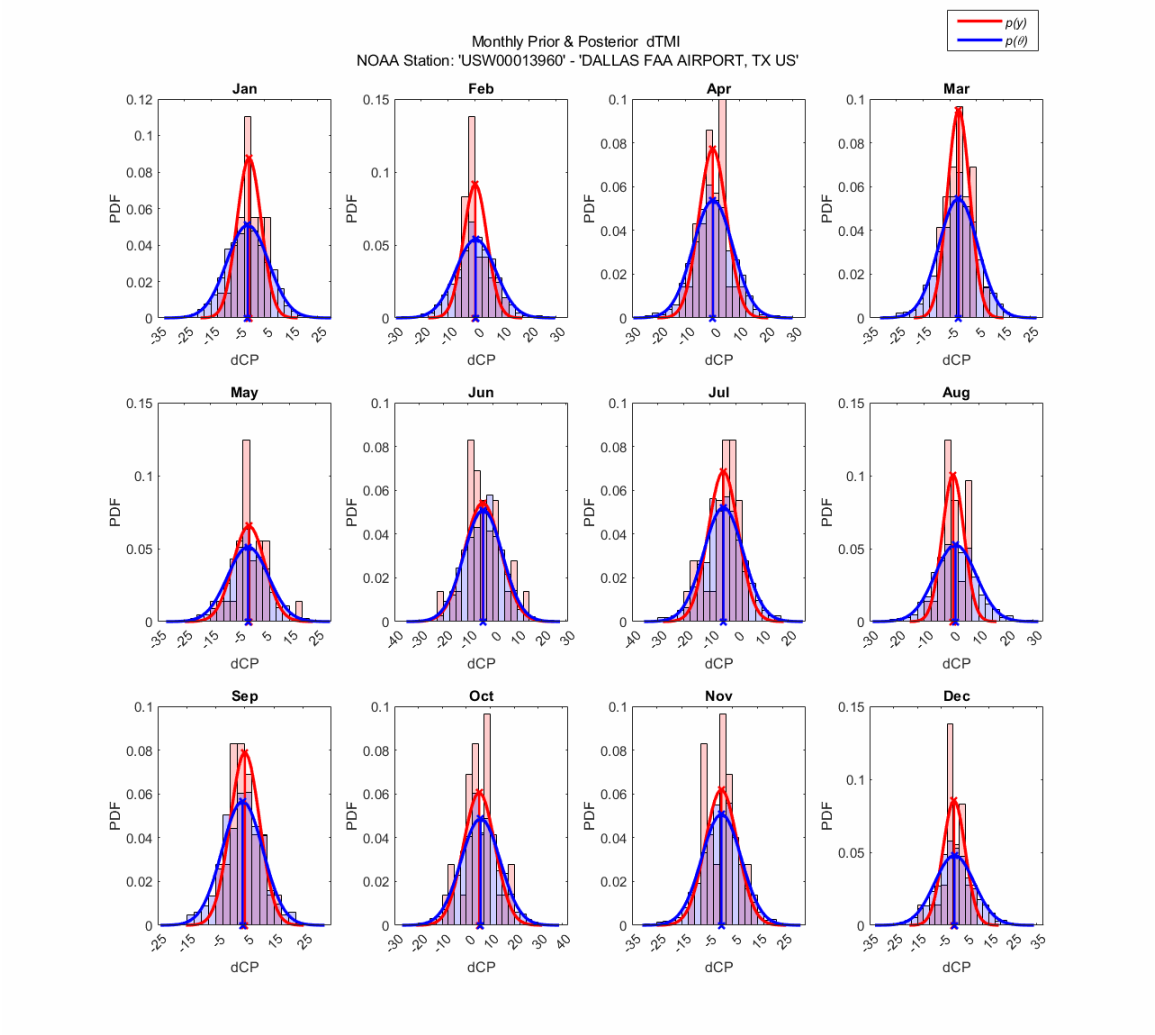

Figure 9-16 Histograms of Prior and Posterior (forecasted) Monthly Change in TMI for the Dallas, TX Validation Study Site from 03/2017 to 03/2022.

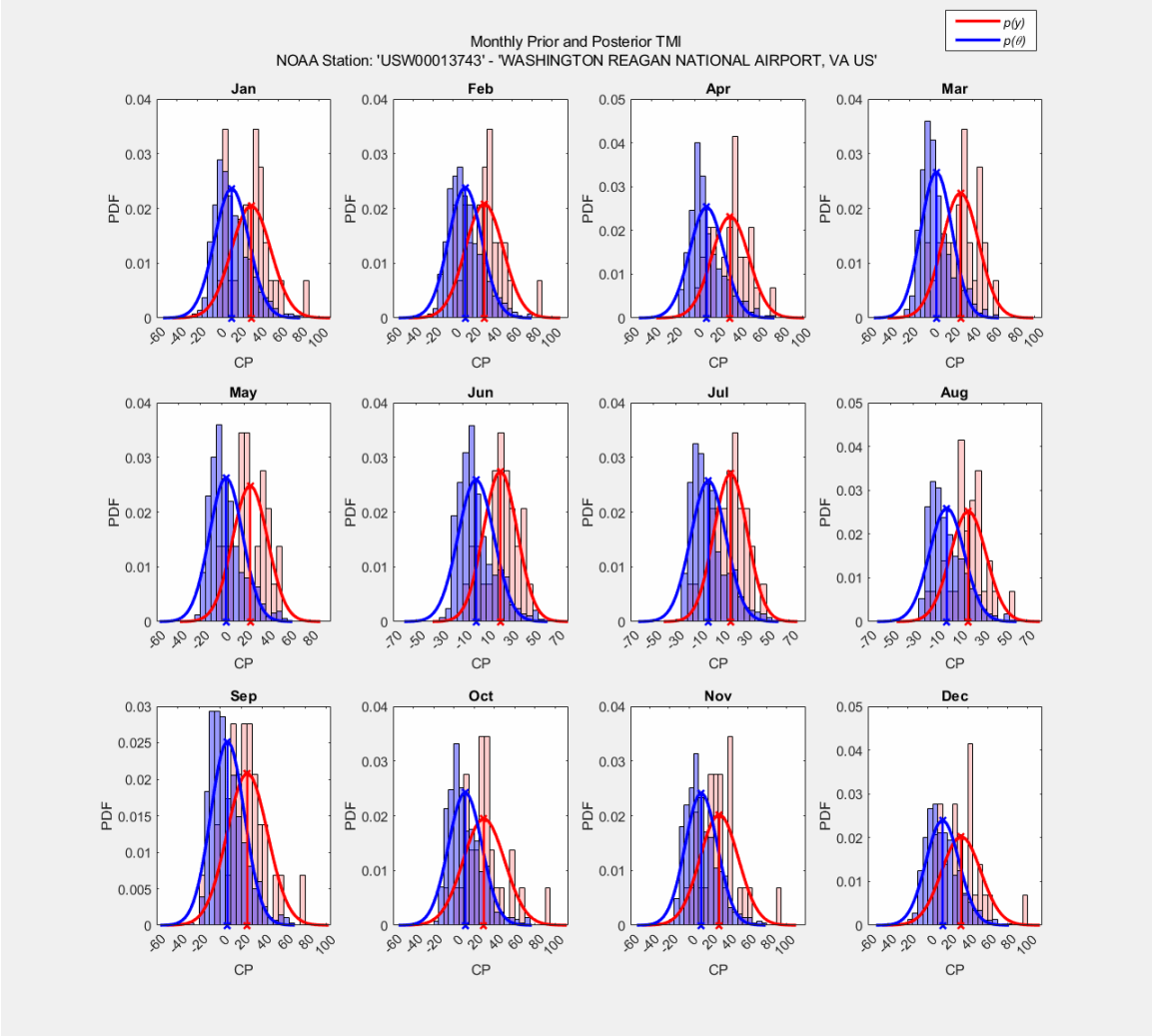

Figure 9-17 Histograms of Prior and Posterior (forecasted) TMI for the Arlington, VA Validation Study Site from 03/2017 to 03/2022.

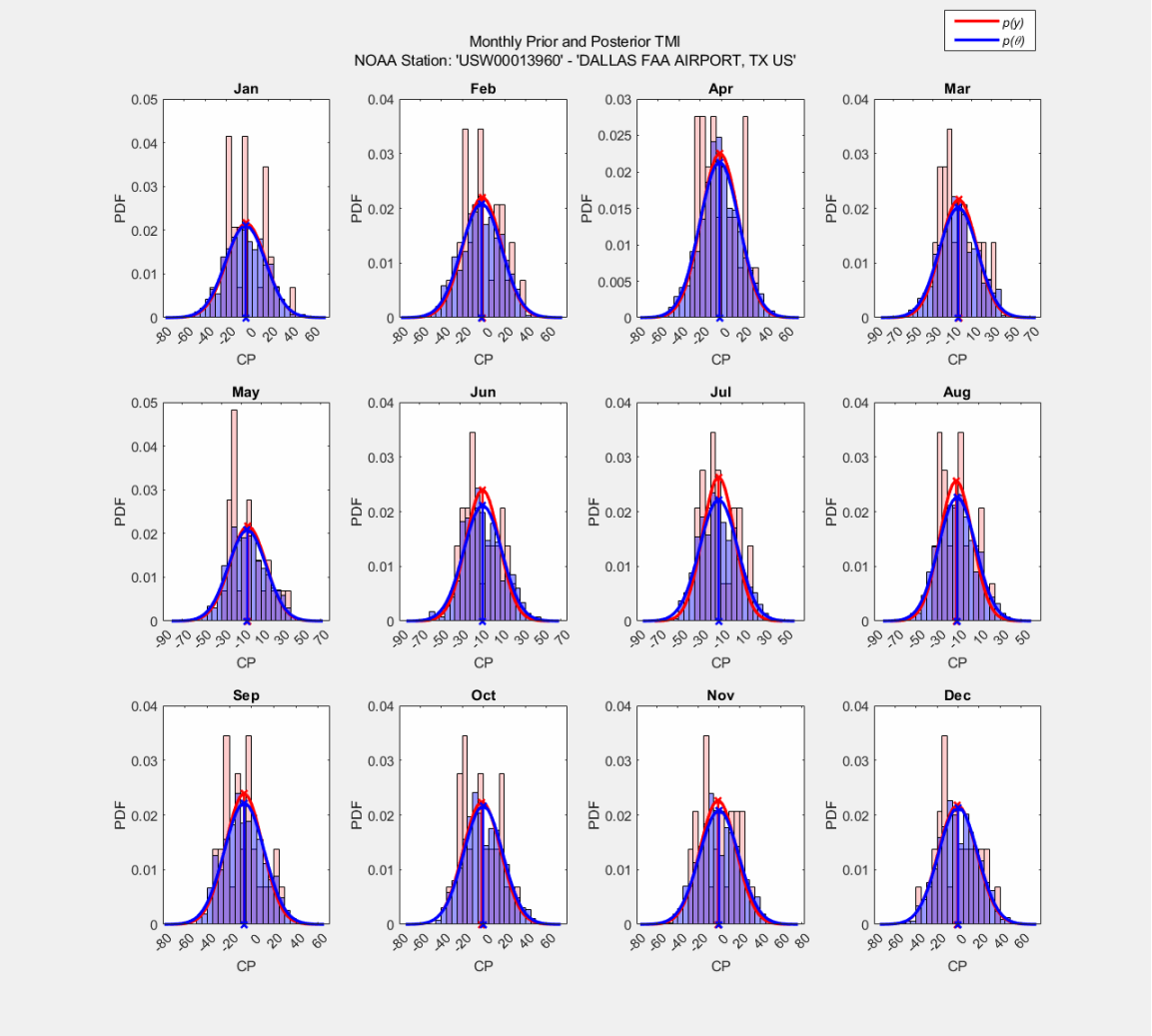

Figure 9-18 Histograms of Prior and Posterior (forecasted) TMI for the Dallas, TX Validation Study Site from 03/2017 to 03/2022.

The *dTMI* histograms for the Arlington study location indicate that posterior data produced by the Bayesian TMI forecast model resulted in a reduction of variability of the monthly data compared to the priors, which can be observed by the narrower distribution fit and increased frequency of values near the mean (i.e., increased kurtosis). This is not a favorable result as the forecast model under predicts the variability of the historical data. The TMI histograms for the Arlington study site display another unfavorable outcome of the forecasted data as the average of each monthly posterior distribution noticeably differs (more positive) than the average of the prior distributions. This indicates that the forecast model is not producing data which follows the mean of the historical prior data. These two lacks of fits between the forecasted posterior data and the historical prior data may be what caused the lack of fit of the extreme event shown previously in Figure 4-5.

In contrast, the prior and posterior histograms for the *dTMI* values for the Dallas, TX study location indicate that the Bayesian TMI forecast model is over predicting the variability of the prior data

(decreased kurtosis) for most of the months; and the distributions of the TMI prior and posterior data show that the model is producing nearly equivalent means for each of the monthly priors.

9.9 Stability of the Bayesian TMI Forecast Model

The stability of the Bayesian TMI Forecast Model was tested by performing forecast simulations for differing starting seasons/dates, over varying forecast durations (2 to 20 years), for the five locations used in the validation study. The graphical results of the stability analyses are presented in Appendix F. In summary, the forecast model performed sufficiently and efficiently regardless of the initial conditions and the duration of the forecast period. However, the stability of the model was not tested using priors with limited or missing data, or at locations where the average TMI is near the limits of either -100 or 100.

9.10 Potential Future Improvements to the Bayesian TMI Forecast Model

The research efforts produced useful frameworks for the stochastic forecast of the climatic parameter TMI using time-series and Bayesian Inference techniques Although the proposed model produced promising results for the sites explored in the validation study, which has potential for several further improvements.

- The inclusion of multiple weather station data should be incorporated into both the deterministic and the stochastic models. For the deterministic model, a decision would have to be made to use the average monthly data, or another statistically representative monthly value. Although it is not a straightforward analysis, the most conservative approach would be to use the monthly data which results in the greatest monthly changes and/or seasonal variations, regardless of the location of the weather station (assuming only weather stations near the site that are chosen).
- Improvement and optimization of the Bayesian forecast model for the climatic parameter TMI to include an adaptive Langevin Markov Chain (LMC) or a Hamiltonian Markov Chain (HMC) which incorporates a physics-based approach to control the stability and limit the random walk potential of the simulated time-series by representing the MCMC framework as energy equations (potential and kinetic). The HMC framework also includes a leap-frog step which can significantly optimize the computation time of the MCMC simulation.
- Evaluation of extreme climate events (in perspective of TMI) with the potential development of a Bayesian probability model which can force the forecasted TMI values to include some percentage and probability of extreme events into the forecasted data.

9.11 Limitations of the Bayesian TMI Forecast Model

The author recommends that the models be treated as preliminary framework which needs further optimization, validation, and sensitivity analyses, the following efforts should be performed as part of future research work:

- As displayed in the outcome of the Arlington, VA validation study, the proposed Bayesian TMI forecast model has potential to miss extreme events which were not characterized by the 30 years of prior climate data.

The Bayesian TMI forecast model presented herein is programmed to produce forecasts which sufficiently represent the variability and volatility of the prior data without "walking" too far from the prior distributions. If a more conservative approach is warranted which encompasses some pre-defined increase in the variability/volatility of the forecasted data, the tuning criteria can be increased by either increasing the initial tuning factor to be greater than 2.4. An additional stability study should be performed in such a case.

9.12 References

Federal Highway Administration – FHWA (1995) LTPP seasonal monitoring program site installation and initial data collection section 481068. FHWA, Paris, TX

Gelman, A., Carlin, J. B., Stern, H. S., Dunson, D. B., Vehtari, A., and Rubin, D. B. (2013). Bayesian Data Analysis. Chapman & Hall/CRC.

Haario, H., Saksman, E., & Tamminen, J. (2001). An Adaptive Metropolis Algorithm. Bernoulli, 7(2), 223-242.

Hasting, W. K. (1970). "Monte Carlo sampling methods using Markov Chains and their applications." Biometrica, 57(1), 97.

Metropolis, N., Rosenbluth, A. W., Rosenbluth, M. N., Teller, A. H., and Teller, E. (1953). "Equation of State Calculations by Fast Computing Machines." The Journal of Chemical Physics, 21(6), 1087–1092.

Mitchell, P.W. (1979). The Structural Analysis of Footings on Expansive Soil. Newton: Kenneth W.G. Smith& Associates.

Mitchell, P.W. (1980). The Concepts Defining the Rate of Swell of Expansive Soils. *Proceedings of the 4th International Conference on Expansive Soils*. Denver, USA. Volume 1, pp 106-116.

Montgomery, D. C., Jennings, C. L., & Kulahci, M. (2016). Time Series Analysis and Forecasting. Hoboken, NJ: John Wiley & Sons, Inc.

Olaiz, A.H.; Singhar, S.H.; Vann, J.D. & Houston, S.L. (2016). Comparison & applications of the Thornthwaite moisture index using GIS. *Proc. of the 2nd PanAm Conf. on Unsaturated Soils, Dallas, TX, Vol. 1*, ASCE.

Olaiz, A. H., Mosawi, M., & Zapata, C. (2021). An improved framework for volume change of shrink/swell soils subjected to time-varying climate effects. (F. M. T.M.P. Campos, Ed.) Soils and Rocks - Special Issue: Unsaturated Soils, 44(3), 1-14.

Perera, Y. Y. (2003). Moisture Equilibria beneath Paved Areas. Ph.D. Dissertation, Arizona State University, Arizona, U.S.A.

Vann, J.D., & Houston, S. (2021). Field Suction Profiles for Expansive Soil. Journal of Geotechnical and Geoenvironmental Engineering, 147(9), 04021080. https://doi.org/10.1061/(ASCE)GT.1943-5606.0002570.

Witczak, M.W., Zapata, C.E. and Houston, W.N. (2006). Models Incorporated into the Current Enhanced Integrated Climatic Model: NCHRP 9-23 Project Findings and Additional Changes after Version 0.7. Final Report. Project NCHRP 1-40D.